NOTES AND CORRESPONDENCE

Interplay of Resonant and Quasi-Resonant Interaction of the Directional Ocean Waves

TAKUJI WASEDA

Department of Ocean Technology Policy and Environment, Graduate School of Frontier Sciences, University of Tokyo, Kashiwa, and Research Institute for Global Change, JAMSTEC, Yokohama, Kanagawa, Japan

TAKESHI KINOSHITA

Institute of Industrial Science, University of Tokyo, Tokyo, Japan

HITOSHI TAMURA

Research Institute for Global Change, JAMSTEC, Yokohama, Kanagawa, Japan

(Manuscript received 18 September 2008, in final form 28 March 2009)

ABSTRACT

Recent experimental study of the evolution of random directional gravity waves in deep water provides new insight into the nature of the spectral evolution of the ocean waves and the relative significance of resonant and quasi-resonant wave interaction. When the directional angle containing half the total energy is broader than ~20°, the spectrum evolves following the energy transfer that can be described by the four-wave resonant interaction alone. In contrast, in the case of a directionally confined spectrum, the effect of quasi-resonant wave–wave interaction becomes important, and the wave system becomes unstable. When the temporal change of the spectral shape due to quasi resonance becomes irreversible owing to energetic breaking dissipation, the spectrum rapidly downshifts. Under such extreme conditions, the likelihood of a freak wave is high.

1. Introduction

Advancement in the understanding of freak waves has led people to rethink the nature of the ocean waves in deep water. The description of the ocean waves, by a self-similar wave spectrum that downshifts due to four-wave resonant interaction, seems robust. However, the generation of the freak wave is suggested to be associated with the abnormally narrow wave spectrum. Recent numerical and experimental studies provide evidence that the quasi-resonant interaction is at work when the angular distribution and frequency bandwidth of the wave spectrum is narrow (Onorato et al. 2002; Janssen 2003; Onorato et al. 2004; Soquet-Juglard et al. 2005; Gramstad and Trulsen 2007; Waseda et al. 2009; Onorato et al. 2009). These studies dealt with artificially generated abnormal waves, such that the initial spectral shape deviates considerably from the waves typically found in the ocean.

This note is a complement to Waseda et al. (2009), which illustrates in detail the long-term evolution of wave statistics of the random directional wave, including directionally broad realistic spectra. They present evidence that the kurtosis of the surface elevation time series, representing the intensity of the quasi-resonant interaction, decreases as the directional spreading increases. Following this study, we investigated the evolution of the wave spectra to elucidate the relative significance of the resonant and quasi-resonant interaction.

Fundamental processes of the quasi-resonant interaction are depicted in the evolution of the unstable Stokes wave. The spectral downshifting of the unstable

Corresponding author address: Takuji Waseda, Department of Ocean Technology Policy and Environment, Graduate School of Frontier Sciences, University of Tokyo, 5-1-5 Kashiwanoha, Kashiwa, Chiba 277-8563, Japan.
E-mail: waseda@k.u-tokyo.ac.jp

DOI: 10.1175/2009JPO4147.1

Stokes wave has been studied extensively in both conservative and nonconservative frameworks (Trulsen and Dysthe 1997 and references therein). Melville (1982) provided the first experimental evidence of the permanent spectral downshifting accompanied by breaking dissipation, which was later elaborated by Tulin and Waseda (1999). Numerous studies of the unstable Stokes wave using the nonlinear Schrödinger equation and its variation suggest that the introduction of weak dissipation inevitably causes the spectrum to downshift (e.g., Hara and Mei 1991), whereas Trulsen and Dysthe (1997) suggested that downshifting can occur even without dissipation when the effect of directional spreading is taken into consideration. Note, however, that the downshifting discussed by Trulsen and Dysthe (1997) is rather slow because it is a result of the nonlinear energy transfer due to four-wave resonance, which has a time scale of the order of a few hundred wave periods.

A typical structure of the nonlinear transfer function for young ocean waves indicates that the shift of energy to lower frequencies is always accompanied by the leak of energy to higher frequencies to conserve wave momentum (Hasselmann et al. 1985). For the case of a unidirectional random wave, four-wave resonance cannot occur but an apparent shift of the spectral peak due to quasi resonance is possible with the development of a higher frequency spectral tail (e.g., see Janssen 2003). However, a recent study by Stiassnie et al. (2008) suggests that the evolution of a unidirectional random wave may undergo a recurrence so that eventually the initial energy spectrum is retrieved. Therefore, it is conjectured that a permanent downshift is possible only when energy and momentum are not conserved.

We extended these pioneering works and studied the evolution of random directional wave in a laboratory wave tank both with and without energetic breakers (Waseda et al. 2009). From this study, we hypothesize that, for a directionally narrow wave spectrum, permanent downshifting occurs as a result of quasi-resonant interaction and the breaking dissipation but, for the directionally broad wave spectrum, frequency downshift occurs due to four-wave resonance even without breaking dissipation. The availability of the broad [e.g., Hwang and Wang (2001) directional distribution] and narrow spectra in a laboratory setting allowed us to identify the relative significance of the two downshifting mechanisms for distinct angular distributions.

In section 2, the experimental settings will be described briefly. The spectral evolution will be shown for the selected experimental cases in section 3, and the evolution of the spectral properties will be discussed in section 4. A summary follows in section 5.

2. Experimental setting

The experimental setting is illustrated in detail in Waseda et al. (2009). The experiments were conducted using the Ocean Engineering Tank (50 m long, 10 m wide, and 5 m deep) of the Institute of Industrial Science of the University of Tokyo (Kinoshita Laboratory and Rheem Laboratory). The directional wave was generated by a segmented plunging wave generator (32 plungers across 10 m),

$$S(\omega, \theta) = F(\omega)G(\theta; \omega). \quad (1)$$

Both the frequency spectrum $F(\omega)$ and directional spreading function $G(\theta; \omega)$ are arbitrarily determined, and the spectrum is equipartitioned in energy for 1024 random wave components. For all of the cases analyzed, the frequency spectrum is given by the Joint North Sea Wave Atmosphere Project (JONSWAP) spectrum:

$$S(\omega) = \alpha g^2 \omega^{-5} \exp\left[-\frac{5}{4}\left(\frac{\omega}{\omega_p}\right)^{-4}\right] \gamma^{\exp[-(\omega-\omega_p)^2/(2\sigma^2\omega_p^2)]}, \quad (2)$$

and one of the following directional distribution functions; the Mitsuyasu-type directional spreading function:

$$G(\theta) = G_n \cos^n(\theta); \quad (3)$$

the Hwang and Wang (2001) distribution function; and the bimodal distribution function [refer to Waseda et al. (2009) for details]. Controlling parameters α, γ, and n, we have generated waves with a variety of wave steepness, frequency bandwidth, and directional spreading [wave steepness $0.05 < \varepsilon(\equiv ak) < 0.11$, with directional spreading up to 36°; frequency bandwidth $0.2 < \delta k/k < 0.6$; and significant wave height 3–6 cm] for peak frequency 1.2389 Hz or 7.784 rad s^{-1} (wavelength 1 m, $T_{1/3} = T_p/1.05 = 0.7626$ s).

In a typical arrangement of the experiments, the wave wires are placed 2.3 m from the sidewall at 5-m intervals along the tank to monitor the evolution of the wave spectrum and other statistical parameters. In addition, an array of four to six wires, used in combination to measure the directional spectrum, can be located at arbitrary locations in the tank. To quantify the observed directional distribution, the inverse of the normalized directional distribution A will be estimated from the measured directional spectrum:

$$A^{-1} = \int_{-\pi}^{\pi} K(\theta; \omega)\, d\theta; \quad \int_{-\pi}^{\pi} AK(\theta; \omega)\, d\theta = 1, \quad (4)$$

where $AK(\theta; \omega) \equiv G(\theta; \omega)$ and $\max[K(\theta; \omega)] = 1$ (see, e.g., Babanin and Soloviev 1998). The directional spectrum

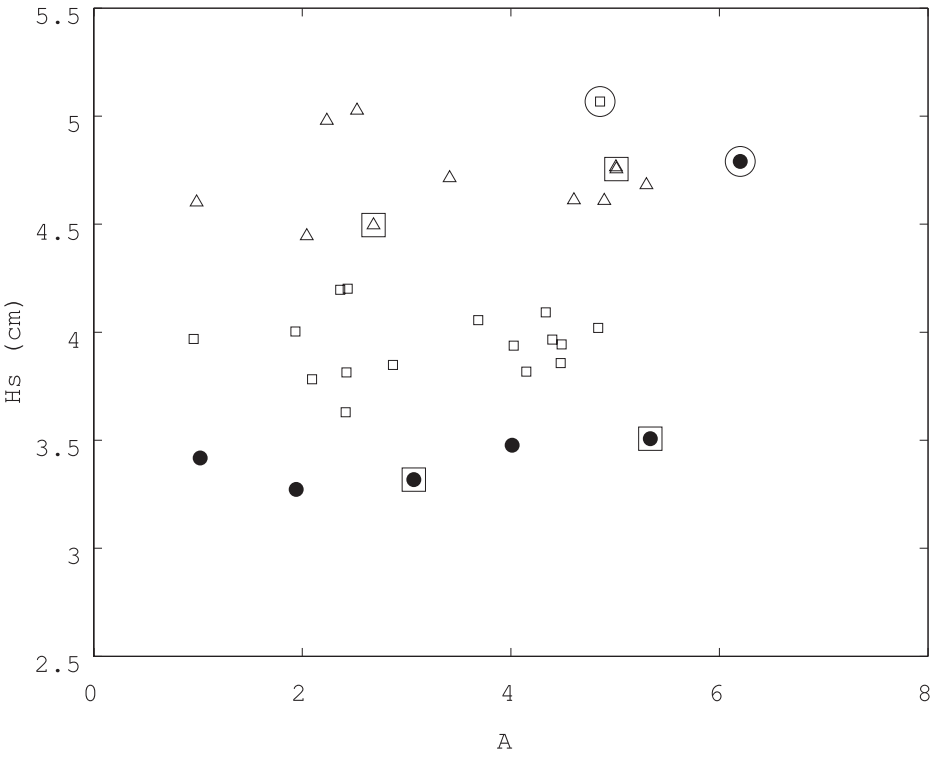

FIG. 1. Significant wave height H_s at 15-m fetches plotted vs directional spreading A for all the cases. The cases are categorized into three ranges of experimental settings: $H_s = 5.0$ (triangle), $H_s = 4.15$ (square), and $H_s = 3.50$ (solid circle). Strong breakers were visible for cases when the observed H_s were more than 4.5 cm; gentle breakers were visible for the observed $H_s \sim 4$ cm; and no breakers were visible for cases with observed $H_s \sim 3.5$ cm. Spectral evolution is shown in Fig. 2 for cases indicated by a square surrounding the symbol. Circles surrounding the symbols indicate unidirectional cases.

$S(\omega, \theta)$ was estimated using the wavelet detection method (Donelan et al. 1996).

More than 30 cases of directional spectra with different energy levels, directional distributions, and frequency bandwidths were generated. The observed significant wave heights at 15-m fetch are plotted against the observed directional distribution A [Eq. (4)], indicating the range of parameters of the conducted experiments. Those cases can be categorized into three groups by the values of the imposed significant wave height (Fig. 1). The largest case ($H_s = 5.0$ cm; △) involved visibly energetic wave breakers. Wave breaking was still observed for the intermediate case ($H_s = 4.15$ cm; □), but no wave breaking was visible for the least energetic case ($H_s = 3.5$ cm; ●), except for the unidirectional case indicated by a larger circle surrounding the symbol. In the following sections, selected cases (denoted by a square surrounding the symbols: △ and ●) are analyzed further to show their distinct character of the spectral evolutions. Cases with strong breakers ($H_s = 5.0$ cm; △) will be analyzed to investigate the downshifting mechanism driven by quasi resonance and breaking dissipation, and cases with no visible breakers ($H_s = 3.5$ cm; ●) will be analyzed to evaluate the relative significance of the resonant and quasi-resonant interaction as a function of the directional distribution.

3. Spectral evolution

Typical evolution of the directionally narrow spectra is shown in Figs. 2a and 2b. Shapes of the imposed directional spectrum are identical ($\gamma = 3.0$, $n = 25$) but the significant wave height differs ($H_s = 3.5$ and 5 cm or $ak = 0.055$ and 0.08). The frequency bandwidth is ordinary because typical oceanic values of γ are considered to be ~3.3. However, the directional spreading ($n = 125$) is abnormally narrow; half of the energy is contained within ±3.5° of the mean direction. For both cases (Figs. 2a,b) downshifting of the spectral peak at its developed stage (40-m fetch) is evident. Because the directionality is extremely narrow, we speculated that this downshifting is a result of the quasi-resonant nonlinear interaction rather than the exact resonant interaction. The rate of frequency downshift within 40 wave

periods, or so, is a few percent for the case without visible breakers (H_s = 3.5 cm, Fig. 2a) and ~5% for the case with strong breakers (H_s = 5 cm, Fig. 2b). The downshifting rate is much faster than that owing to a conservative weakly nonlinear process alone.

On the contrary, when the directional distribution is broad (27.8°, ±13.9° or $1/A \sim 0.5$), downshifting of the spectral peak is not apparent. In Fig. 2, the spectral evolution for cases H_s = 3.5 (Fig. 2c) and 5 cm (Fig. 2d) are compared ($\gamma = 3.0$, $n = 10$). Unlike the directionally narrow cases, the spectral peak remains nearly the same, regardless of whether the strong breaker was present or not. Thus, the rapid downshifting caused by the quasi-resonant interaction seems absent for these cases. However, there is a signature that the higher frequency side of the spectral energy decreases, whereas the lower frequency side increases (e.g., Fig. 2d).

To quantify this energy shift, we estimated the mean frequency, defined as the first moment of the energy spectrum normalized by the total energy:

$$\overline{\omega} = 2\pi\overline{f} = \frac{\int \omega F(\omega)\, d\omega}{\int F(\omega)\, d\omega}. \tag{5}$$

To the lowest order $\overline{\omega}/g$ is the ratio of wave momentum and wave energy.[1] Unlike the spectral peak that exhibits a discrete transition to a lower frequency, the mean frequency $\overline{\omega}$ makes a smooth transition. In Fig. 3, the evolution of the mean frequency $\overline{\omega}$ is shown for the cases of the same wave conditions as in Fig. 2 ($\gamma = 3.0$, $n = 10$ or 125, and H_s = 3.5 and 5 cm). Comparison of the mean frequency $\overline{\omega}$ (Fig. 3) suggests that, even if the spectral peak frequency is unchanged, the spectral moment decreases because the spectral shape has changed accordingly. The shift of peak frequency and change of mean frequency should be distinguished. From Hasselmann's theory, which is based on the Eulers equation, both momentum and energy are conserved; in that case, the mean frequency defined as (5) will remain unchanged, even if the spectral peak downshifts owing to energy transfer among spectral components. However, in most realistic situations, dissipation cannot be neglected and, therefore, the mean frequency will change.

Downshifting of the directionally broad spectrum occurs as a result of the resonant four-wave interaction among spectral components. The nonlinear transfer of energy causes the spectral peak to downshift with duration and fetch, whereas the spectral tail equilibrates. From observation, theory, and numerical/physical experiments, the equilibrium tail of ocean waves is suggested to follow the power laws: ω^{-4} or ω^{-5}. The former tail forms due to nonlinear resonant interaction and the latter forms when breaking dissipation becomes dominant. Therefore, we may test whether the nonlinear resonant interaction is at work or not by looking into the development of the high-frequency equilibrium tail of the spectrum in the tank. The saturation spectra $B(\omega) = \omega^5 F(\omega)$ (Fig. 4) tend to equilibrate for all cases extending beyond the generated frequencies (2.5 Hz). The development of the spectral tail is likely a result of the energy cascade due to nonlinear interaction. However, a closer look at the high-frequency tail suggests that the resulting slope varies with directional spreading of the spectrum. The maintenance of the equilibrium tail is one of the roles of the resonant interaction and that will be discussed more in the next section.

4. Discussion

a. Spectral downshifting due to strong nonlinearity

In the ocean, spectral downshifting is considered to occur as a consequence of the resonant four-wave interaction, and its rate depends on the spectral shape. The four-wave interaction is most efficient for a combination of resonant waves that includes two waves propagating at angles ~11.5° and −33.6° to the other waves [e.g., discrete interaction approximation (DIA), Hasselmann et al. (1985)]. As we will show in section 4c, when the wave spectrum becomes extremely narrow in direction, the resonant energy transfer becomes less effective. The directional spreading of the spectrum shown in Figs. 2a,b is extremely narrow (~7° ± 3.5° or $1/A \sim 0.25$); therefore downshifting due to resonant interaction is unlikely. However, both steepness cases ($\gamma = 3.0, n = 125$; H_s = 3.5 and 5 cm) downshift, and the rate is higher for the larger initial steepness case.

[1] The interpretation of the numerator of (5) as the wave momentum is valid only for the unidirectional wave. For the directional wave, the total energy is given as

$$\iint F(\omega)G(\theta;\omega)\, d\theta\, d\omega = \int F(\omega)\, d\omega,$$

where $\int G(\theta;\omega)\, d\theta = 1$. The momentum in the mean propagating direction is given as

$$\iint (\omega/g)F(\omega)\cos\theta G(\theta;\omega)\, d\theta\, d\omega = \int (\omega/g)F(\omega)\, d\omega \times \left[\int \cos\theta G(\theta;\omega)\, d\theta\right].$$

The term in the bracket is not unity and will introduce error, in estimating the wave momentum in the mean propagating direction, if (5) is used. For a directional spreading (3), the error is estimated to be around 5% for $n = 10$ and rapidly diminishes as the spectrum narrows (1% for $n = 50$; 0.5% for $n = 100$; and 0.2% for $n = 250$). The downshift from the initial $\overline{\omega}$ in Fig. 3 for $n = 125$ is about 5%. The change in the directional spreading down the tank is minimal and that alone cannot explain the reduction of $\overline{\omega}$ with fetch.

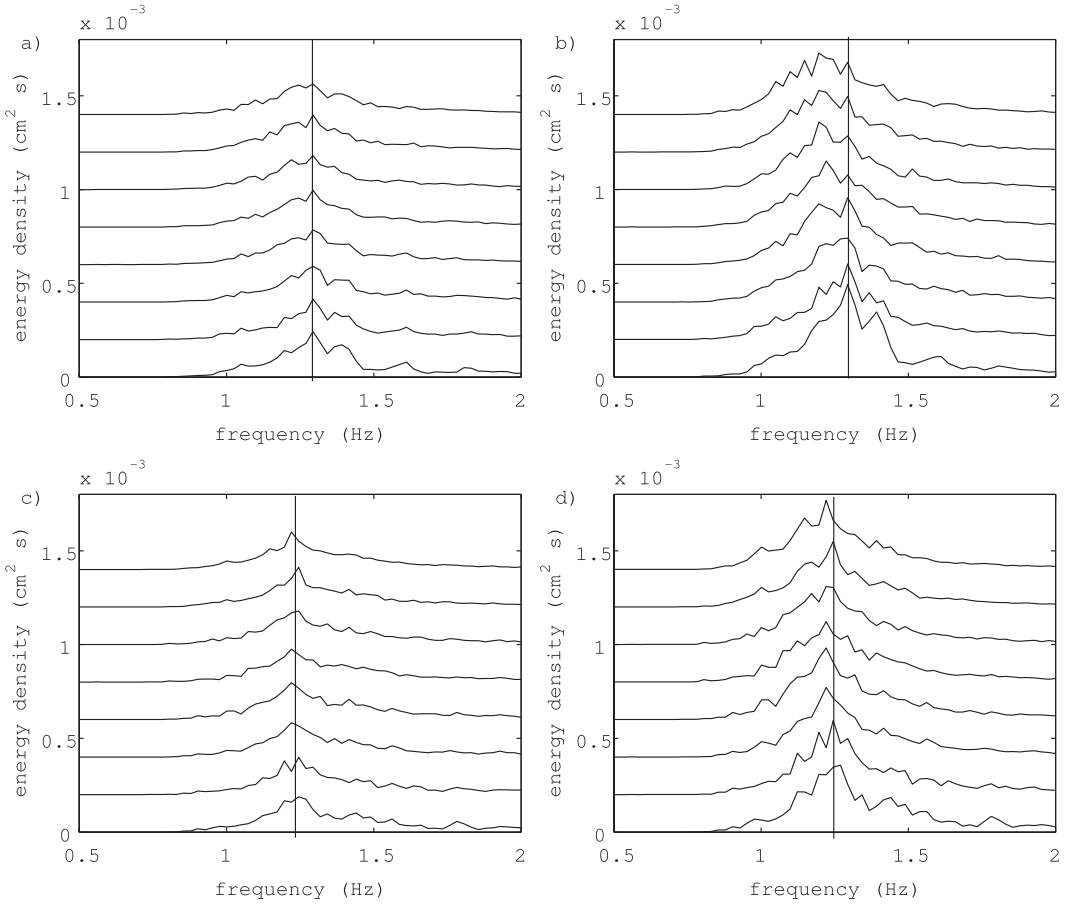

FIG. 2. Spectral evolution at 5-m intervals from 5- to 40-m fetch (energy is artificially shifted): (a) $\gamma = 3.0$, $n = 125$, and $H_s \sim 3.5$ cm ($ak = 0.055$); (b) $\gamma = 3.0$, $n = 125$, and $H_s \sim 5$ cm ($ak = 0.08$); (c) $\gamma = 3.0$, $n = 10$, $H_s \sim 3.5$ cm ($ak = 0.055$); and (d) $\gamma = 3.0$, $n = 10$, $H_s \sim 5$ cm ($ak = 0.08$). The vertical line in each diagram indicates the location of the original spectral peak frequency.

The rate of spectral downshifting is summarized for all experimental cases, including ranges of frequency bandwidth, directional spreading, and steepness (Fig. 5). Regardless of the directionality and frequency bandwidth, the rate of downshifting, defined as the ratio of the mean frequency $\overline{\omega}$ at the developed state (fetch 35–40 m) to the initial state (fetch 10–15 m), decreases with steepness. The magnitude of downshifting, however, is not a straightforward function of directionality and frequency bandwidth. For the largest steepness case ($ak = 0.08$) the rate of downshifting is rather rapid and ~5% reduction of the average frequency occurs within 50 wavelengths, which is certainly not explainable by the resonant interaction alone. According to the four-wave interaction theory, the time scale of the resonant interaction is inversely proportional to the forth power of the steepness—that is, $O(10^4)$ wave periods (Pushkarev et al. 2003). Therefore, the downshifting rate is an increasing function of steepness, but the rate itself from the four-wave interaction theory is much slower than that observed in the tank.

The long-term evolution of the unstable Stokes wave suggests that the downshifting for a unidirectional wave is related to the energy loss due to breaking dissipation. In Fig. 6, the energy loss (defined as the difference of rms elevation between the developed state and initial state) is plotted against steepness. An increasing tendency of the energy loss with steepness is apparent.

The downshifting mechanism based on conservation of energy and momentum was presented by Tulin and Waseda (1999). They have suggested that, because the energetic wave breaking process is rotational, the conservation laws based on potential theory is not valid for the momentum and energy lost during wave breaking. As a result, the wave energy and wave momentum are not conserved before and after wave breaking and an imbalance is inevitable. Here we define an index that represents the imbalance of the lost energy and momentum

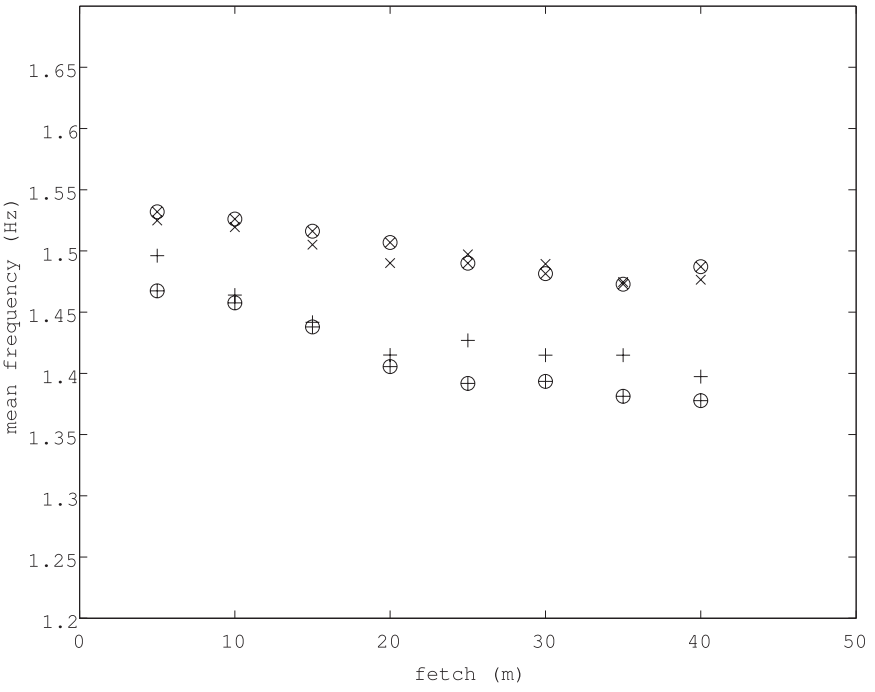

FIG. 3. Evolution of spectral moment or the mean frequency of the spectrum $\bar{f}$ for the cases shown in Fig. 2. Parameters are ⊗: $\gamma = 3.0$, $n = 125$, and $H_s \sim 3.5$ cm ($ak = 0.055$); ⊕: $\gamma = 3.0$, $n = 125$, and $H_s \sim 5$ cm ($ak = 0.08$); ×: $\gamma = 3.0$, $n = 10$, and $H_s \sim 3.5$ cm ($ak = 0.055$); and +: $\gamma = 3.0$, $n = 10$, and $H_s \sim 5$ cm ($ak = 0.08$).

that can be estimated from the experimental results. A set of free waves is considered, whose total energy E_T and momentum M_T are described as

$$E_T = \sum_j E_j; \quad \dot{E}_T = D_b; \quad M_T = \sum_j M_j, \tag{6}$$

where $E_j = c_j M_j = (g/\omega_j)M_j$. Here D_b is the energy loss due to dissipation, c is the celerity, and ω is the angular frequency where subscript j labels each wave component. The rate of change of the mean frequency as defined in (5),

$$\overline{\omega} = \frac{\sum_j \omega_j E_j}{\sum_j E_j} = \frac{\sum_j \omega_j E_j}{E_T} = g\frac{M_T}{E_T}, \tag{7}$$

can be readily derived as

$$\frac{d\overline{\omega}}{dt} = \frac{\overline{\omega}}{E_T}(\overline{c}\dot{M}_T - D_b) \approx \frac{\overline{\omega}}{E_T}\Gamma D_b, \tag{8}$$

where the proportionality of $\overline{c}\dot{M}_T$ and D_b was heuristically assumed; $\overline{c} = g/\overline{\omega}$. Therefore, the downshifting parameter or the imbalance index

$$\Gamma = \frac{d\overline{\omega}}{dt}\frac{1}{\overline{\omega}}\Big/\left(\frac{D_b}{E_T}\right) \equiv \frac{\text{rate of frequency downshift}}{\text{rate of energy loss}} \tag{9}$$

can only be determined empirically. Tulin and Waseda empirically determined that $\Gamma \approx 0.4$ for the case of an unstable Stokes wave with energetic breakers.

Their work is extended here, and Γ is estimated for the random directional wave with an energetic breaker. First, the rate of frequency downshift $(d\overline{\omega}/dt)/\overline{\omega} = d\ln\overline{\omega}/dt$ and the rate of energy loss $D_b/E_T = d\ln E_T/dt$ were estimated by regression; then the value of Γ was obtained as the ratio of the estimated exponents. The result, Fig. 7, suggests that the value of Γ for the unidirectional case is similar to the value of the unstable Stokes wave, but Γ tends to decrease as the directional bandwidth broadens. The value of the estimated Γ does not approach zero and saturates, suggesting that the energy loss and momentum loss cannot balance to equilibrate the spectrum. The source of energy loss is not apparent from this study.

b. The interplay of resonant and quasi-resonant wave–wave interaction without energetic breakers

In Waseda et al. (2009), the probability of extreme wave occurrence, indicated by the magnitude of the

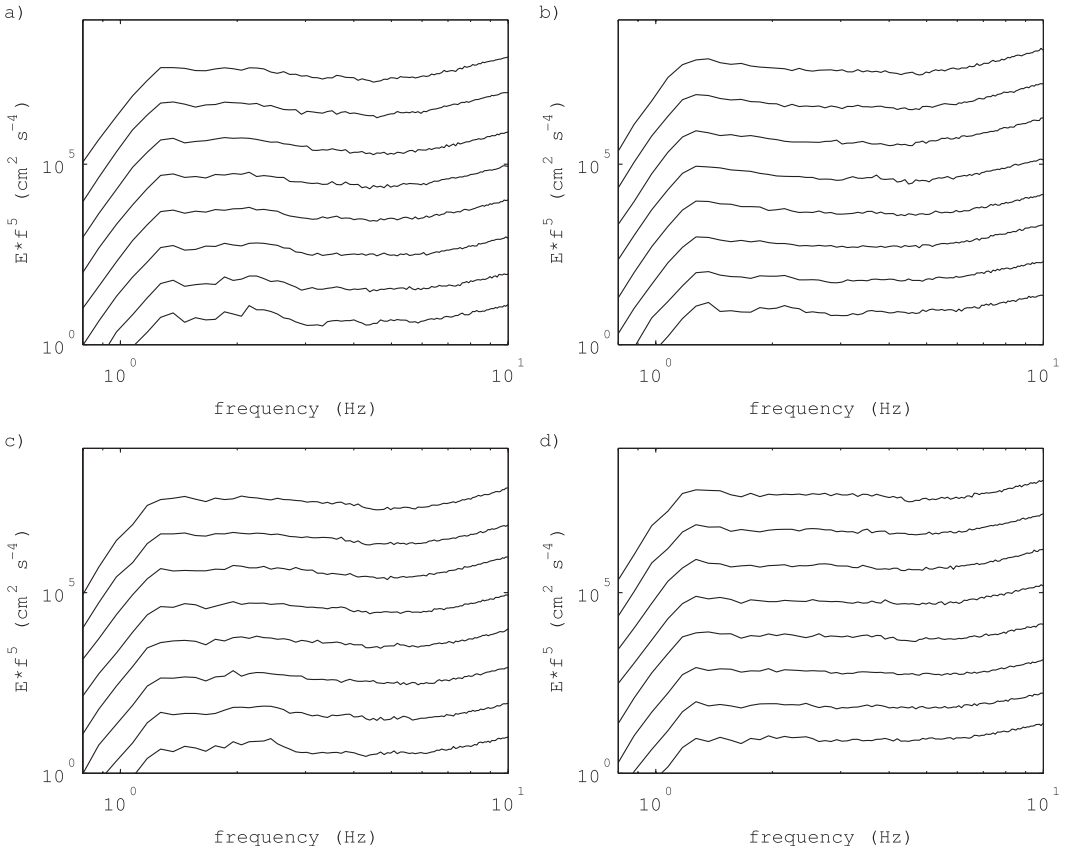

FIG. 4. Evolution of the saturation spectrum at 5-m intervals from 5- to 40-m fetch (the value is artificially shifted) for (a) $\gamma = 3.0$, $n = 125$, and $H_s \sim 3.5$ cm ($ak = 0.055$); (b) $\gamma = 3.0$, $n = 125$, and $H_s \sim 5$ cm ($ak = 0.08$); (c) $\gamma = 3.0$, $n = 10$, and $H_s \sim 3.5$ cm ($ak = 0.055$); and (d) $\gamma = 3.0$, $n = 10$, and $H_s \sim 5$ cm ($ak = 0.08$).

kurtosis, has been shown to increase as the directionality narrows and the quasi-resonant interaction becomes the primary driving mechanism of the spectral evolution. For a broader spectrum, Hasselmann's resonant wave–wave interaction determines the spectral evolution. So, how does the relative significance of the resonant and quasi-resonant interaction alter as directionality changes? We attempt to identify which mechanism is at work by comparing the rate of frequency downshift, energy loss, kurtosis, and downshifting parameter Γ for cases with smallest wave steepness and without visible energetic breakers (Fig. 8).

Remarkably, the downshift of the spectral moment is observed for both broad and narrow directional spectra, but it tends to null around $A = 4$, corresponding to $\sim$20° directional spreading. The kurtosis also starts to increase around $A = 4$. Since the increase of the kurtosis can be attributed to the quasi-resonant interaction (Janssen 2003; Onorato et al. 2004, 2009; Waseda et al. 2009), the frequency downshift for wave spectra narrower than 20° or so indicates the presence of quasi-resonant interaction. The energy loss also minimizes at around $A = 4$, so it seems that the spreading angle of 20° imposes an upper limit to the effectiveness of the quasi-resonant interaction. When the quasi-resonant interaction is combined with energy loss due to breaking dissipation, efficient downshifting occurs, as discussed in section 4a. The cases shown here are all with relatively small steepness, so no energetic breakers were visually observed, except for the unidirectional case (● surrounded by a circle). Insufficient energy loss is likely the reason why the downshift of the spectral peak was not as evident for the case A around 5 (in terms of the cosine to the power of n distribution, $n = 125$). For the directionally narrow random waves, the energetic part of the spectrum becomes spiky (Fig. 2) and the energy seems to cascade down among the peaks—just as in the case of the unstable Stokes wave.

For cases with $A < 4$,that is, for a directionally broad spectrum, the kurtosis remains small (around 3.1), suggesting that the quasi-resonant interaction is inactive. However, the spectrum still downshifts (Fig. 8a), which can only be explained by the presence of the resonant interaction. The presence of resonant interaction is perhaps best evidenced by the development of the

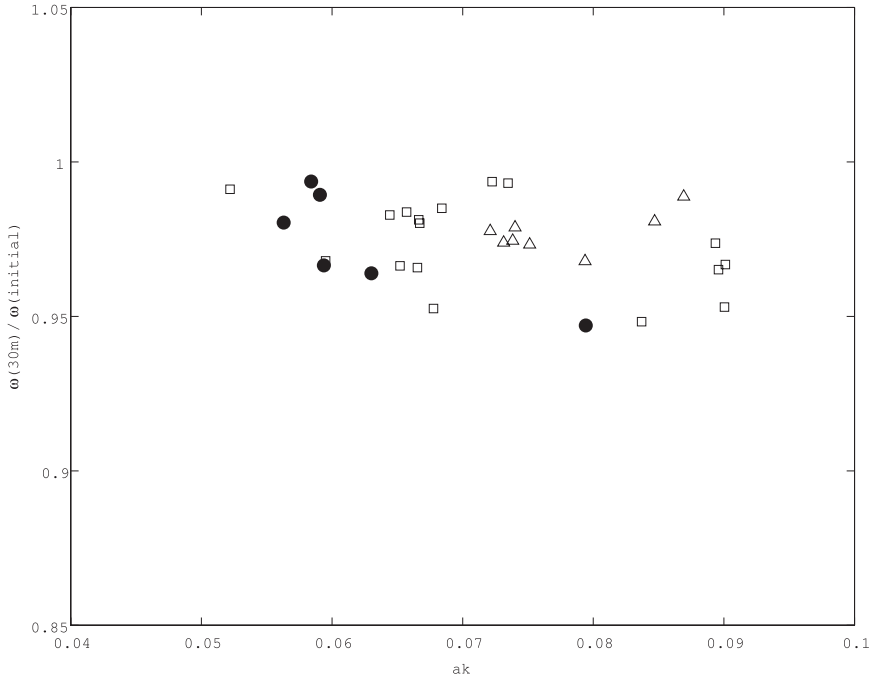

FIG. 5. Frequency downshift plotted against initial steepness for all the cases. The cases are categorized into three ranges of experimental settings as in Fig. 1.

equilibrium spectral tail at high frequencies. Figure 9 displays the spectrum at the early stage (15-m fetch, dashed line) and at the developed stage (40-m fetch, solid line) for two cases with initially identical frequency spectra but with distinctly different directional spreading (Hwang distribution and unidirectional cases). Evidently, the equilibrium range is better developed when the directional distribution is broad enough and the

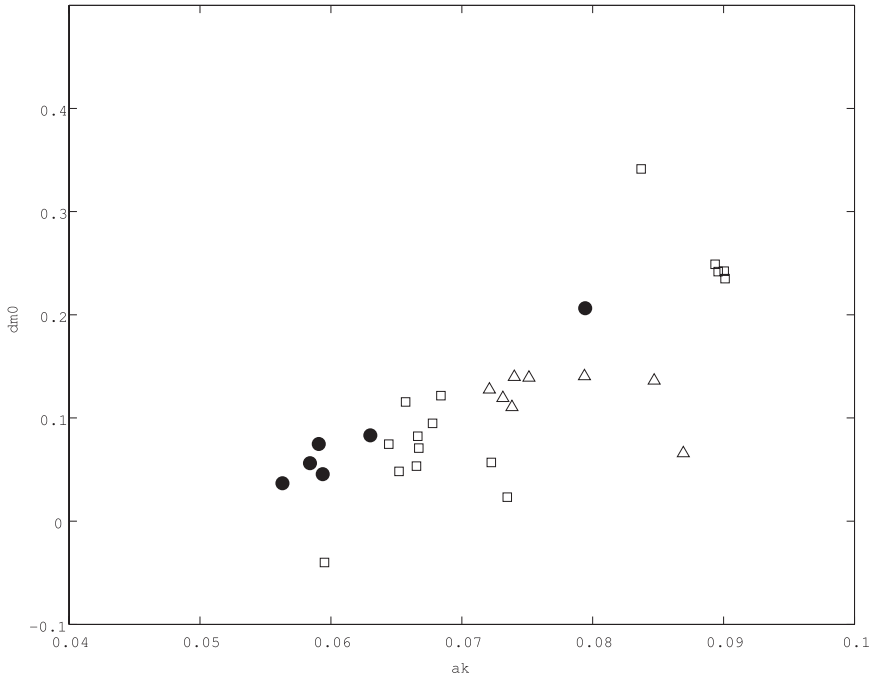

FIG. 6. As in Fig. 5, but for energy loss.

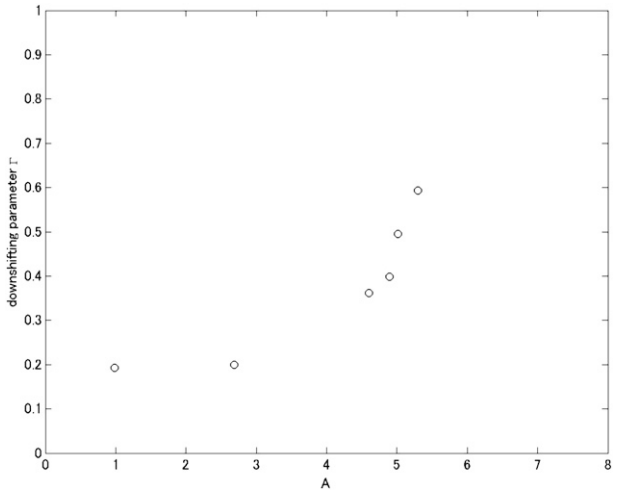

FIG. 7. Downshifting parameter Γ vs directional spreading (A) for cases with energetic breakers.

resonant interaction is more efficient (Fig. 9a). The slope of the equilibrium range tends to approach $\omega^{-4} \sim \omega^{-5}$ at around 2–3 Hz for the directionally broad case, but it is much steeper in the unidirectional case (Fig. 9b). At higher frequencies, where the effect of surface tension is not negligible, the slope of the spectrum does not seem to differ between the directional case and unidirectional case. For both cases, we note the loss of energy in the high-frequency tail and, because strong breakers were absent in the directional case, the loss of energy might result from the energy cascade—inevitable in the establishment of the equilibrium spectrum (Pushkarev et al. 2003). In fact, the loss of energy is not negligible (Fig. 8b) for $A < 4$. However, the downshifting rate is not as efficient as in the unidirectional or directionally narrow case, as one can see from the difference of the values of the downshifting parameter Γ (Fig. 8d). For $A < 4$, the value of Γ is around 0.2, which is much smaller than those values (0.3–0.5) when the directional spread is narrow and the breaking dissipation is evident (see Fig. 7). The establishment of the equilibrium spectrum within 40 wavelengths or so may appear to be too fast for the resonant interaction to work (Badulin et al. 2007). However, the result is consistent with the Tanaka (2001) numerical experiment in which he has shown that the shape of the nonlinear transfer function resembles that of the Hasselmann theoretical solution. The transfer of energy occurs at a much faster rate (20 wave periods) than expected from the homogeneous wave–turbulence theory, $O(10^4)$ (e.g., Badulin et al. 2007). An alternative explanation for the rapid growth of the spectrum is the process of self-stabilization because the initial wave spectrum deviated from the equilibrium condition owing to the truncation of the high-frequency tail and the distortion of the spectrum. We will look into the details of the observed spectral downshifting and the development of the spectral tail in the next section.

c. The role of resonant interaction

It is widely recognized that the equilibrium tail develops and the energy cascades due to four-wave resonant interaction (e.g., Badulin et al. 2007 and references therein). At the same time, the spectral peak downshifts owing to four-wave resonant interaction (Hasselmann et al. 1985). Hwang and Wang (2001) suggested that the ocean wave spectrum is directionally broad near the spectral peak and further broadens at high frequencies and becomes bimodal. Such a directional distribution develops as a result of the four-wave resonant interaction. In our tank experiment, we have artificially generated a wave with a variety of directional distributions from unidirectional to bimodal. The tail of the spectrum immediately develops despite imposing an ω^{-5} spectral tail in the range of frequencies limited to 2.5 Hz or about $2.0\omega_p$ and less. As the waves evolve down the tank, the equilibrium tail develops but with slightly different slope from what was originally imposed (ω^{-5}). The slopes of the equilibrium tail at its most developed stage differ as the directional distribution changes (Figs. 4 and 10). An exponent of $\omega^{-\nu}$ was estimated from the observed wave spectrum for cases without visible breaker in the range from 1.56 to 3.04 Hz (or $1.2 \sim 2.5\omega_p$) including the waves generated by the wave maker (Fig. 10). As the directional distribution broadens (A decreases), the exponent decreases from the imposed value of 5, whereas the exponent increases as the directional distribution narrows (as A increases).

Ocean waves are known to have a self-similar spectral form at its high-frequency regime because of the balance of nonlinear energy transfer, wind input, and energy dissipation. In this tank experiment, we are missing the wind input, and the whitecap dissipation is missing as well, for the condition we have selected to analyze in this section. Thus, the modification of the spectral tail exponent that we observed is likely a consequence of the nonlinear wave interaction. The tank experiment is an initial value problem for which we specify the directional spectrum at one end of the tank. The spectral evolution down the tank is governed by the process of redistributing the wave energy from the most energetic part of the spectrum to the smaller and larger scales. We have observed that, when the directional distribution is sufficiently broad, the equilibrium tail tends to approach ω^{-4} whereas, when the directional distribution is narrow, the tail steepens and approached ω^{-6}. Wind waves at a mature stage are directionally broad and the spectral tail equilibrates to ω^{-4}, whereas at an extremely short fetch,

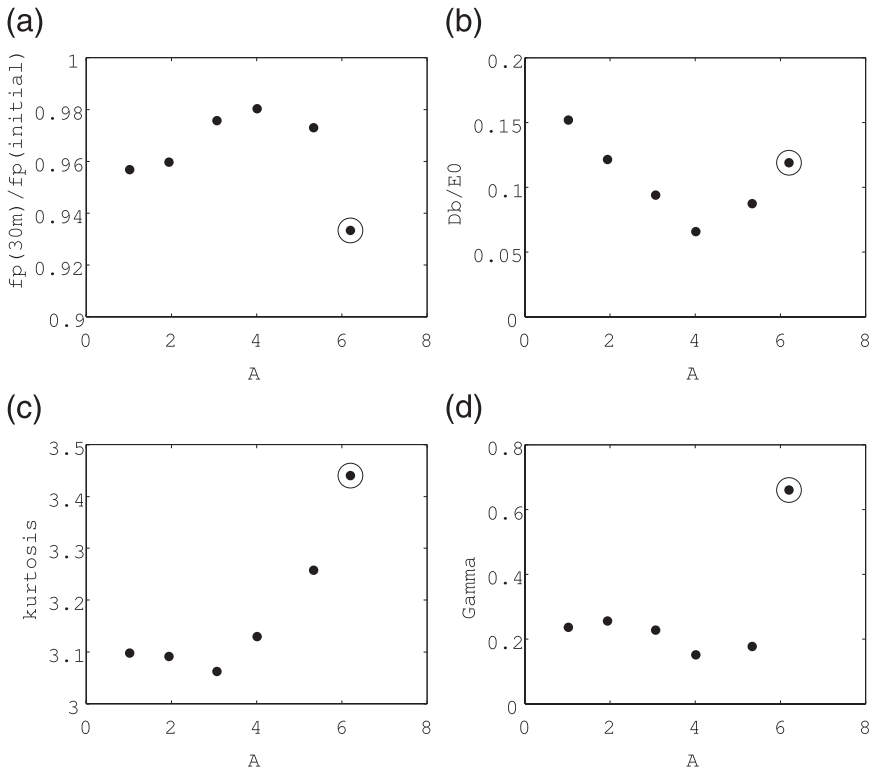

FIG. 8. The (a) rate of frequency downshift, (b) dissipation rate, (c) kurtosis, and (d) the downshift parameter Γ for cases without energetic breakers ($ak \sim 0.055$) vs directional spread A [Eq. (4)]. The larger value of A corresponds to narrower directionality. In ascending order of A, the six distinct directional distributions are bimodal; Hwang; $N = 10$, 50, and 125 in the cos$N$-type distribution; and unidirectional (a dot with a circle). For the unidirectional case H_s is larger than that for the other cases (see Fig. 1).

young wind waves tend to be unidirectional and have a rather steep spectral slope. The tank experiments as conducted, therefore, likely depict realistic processes of the formation of the equilibrium tail for a variety of wind waves, with distinct directional distributions and wave ages, at normal and abnormal/freakish sea states.

For wind waves with distinct directional distributions, we have seen that the rate of frequency downshift changes (section 4). For an extremely narrow directional wave, the frequency downshift occurred as a result of quasi-resonant interaction and whitecap dissipation. For a broader directional spectrum, we conjectured that the downshifting is due to resonant interaction, but its rate slows as the directional distribution narrowed. To prove this hypothesis, we have estimated the nonlinear energy transfer of distinct directional distributions using a simplified, but improved, numerical approximation to the Hasselmann's integral [Research Institute for Applied Mechanics (RIAM) method] (Komatsu and Masuda 1996; Tamura et al. 2008). The initial spectrum was specified by an identical JONSWAP frequency spectrum with $\gamma = 3.0$ with ranges of cosine to the power of n directional distributions [$G(\theta) = G_n \cos^n(\theta)$ for $n = 2$, 100, and 250]. For the broadest case ($n = 2$), the high-frequency energies are shifted to the lower frequencies; therefore the spectrum downshifts (Fig. 11, top). On the other hand, for the extremely narrow directional distribution ($n = 250$), the energy at the spectral peak is shifted toward both higher and lower frequencies and the spectrum does not downshift (Fig. 11, bottom). At an intermediate directional spread ($n = 100$), the spectral downshift prevails but the rate is reduced (Fig. 11, middle). Therefore, the rate of spectral downshifting monotonically decreases as the directional spread narrows and the A increases. Note that, in this numerical simulation, both the spectral peak and mean frequency (5) downshifts because numerical dissipation is present. Now that we have proof that the spectral downshifting due to resonant interaction diminishes as the directional spreading narrows, the corollary is that the spectral downshifting for the narrowest cases in our experiment (Fig. 8a) is a consequence of an alternative mechanism. We have conjectured that to be the quasi resonance augmented by breaking dissipation.

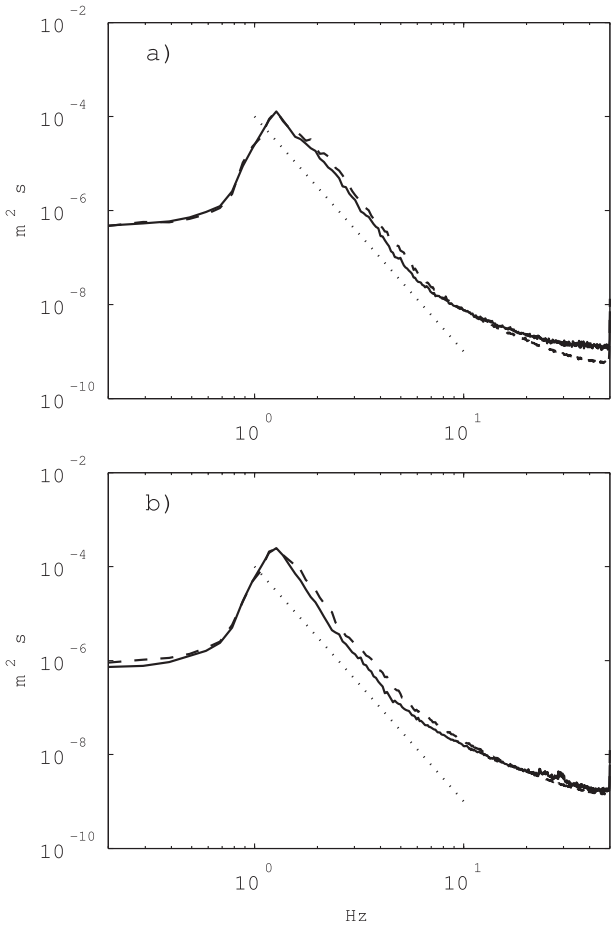

FIG. 9. Development of the high-frequency spectral tail for $\gamma = 3.0$. The equilibrium range develops (solid line at fetch 40 m) from the initial spectrum (dashed line at fetch 15 m): (top) Hwang directional distribution and (bottom) unidirectional. The dotted line is ω^{-5}.

In this section, we have investigated the two roles of resonant interaction in the evolution of the ocean wave spectrum: first, the establishment of an equilibrium high-frequency tail and, second, the downshifting of the spectral peak. Our experimental result provided evidence that these roles are underplayed as the directional distribution narrows. Based on this finding, we can hypothesize that, when the directional distribution is extremely narrow, the high-frequency tail of the spectrum grows steep because the resonant interaction is absent and, in such a case, the downshifting can only occur as a result of the quasi resonance: this is the case when the probability of freak wave occurrence becomes high.

5. Summary

We have attempted to answer the question, ''What is the relative significance of the four-wave resonance and the quasi resonance for the evolution of random directional waves?'' The spectral downshifting for cases with different directionality was examined. Downshifting was found for both the unidirectional case and the broadest case, and the rates were smallest for cases in-between. The change in the wave energy suggests that for the unidirectional case, the instability associated with the imbalance of the energy and momentum loss causes permanent spectral downshifting. On the other hand, when the directionality is broad, instability is absent, as indicated by the small increase of kurtosis from the Gaussian statistics. However, the downshifting is not

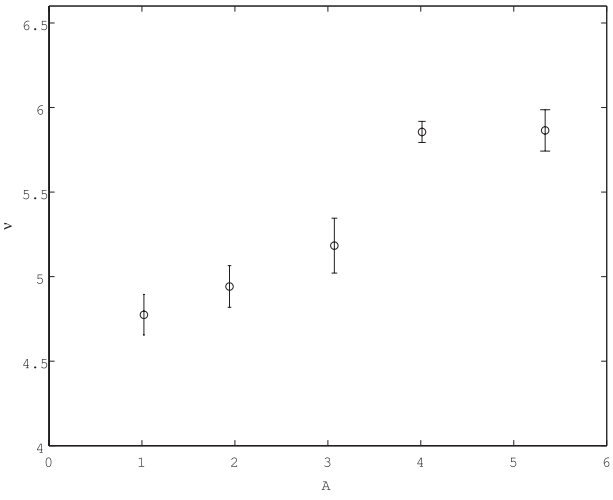

FIG. 10. Estimated exponent of the spectral tail $\omega^{-\nu}$ vs the directional distribution A for the six distinct directional distributions in Fig. 8.

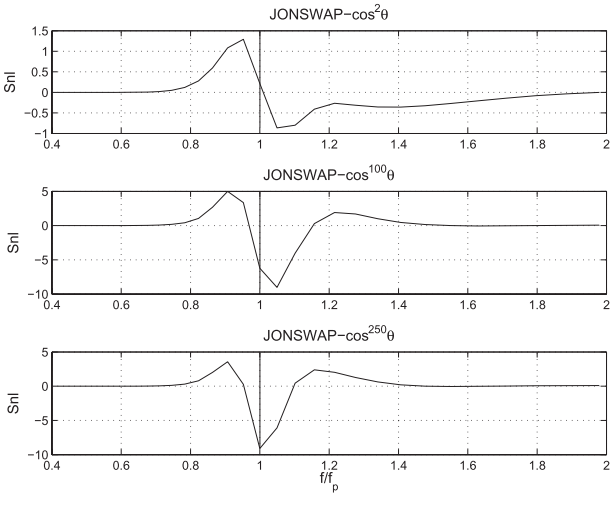

FIG. 11. Nonlinear transfer function for distinct directional distributions: (top)–(bottom) $N = 2$, 100, and 250 in the cos$N$-type distribution. The frequency spectra are identical; JONSWAP type with $\gamma = 3.0$. The nonlinear transfer functions were estimated by the RIAM method.

negligible. The estimated energy–momentum imbalance (i.e., the downshifting parameter Γ) is not as large as in the case of the unidirectional wave. Therefore, there is an indication that the four-wave resonance is effective only when the directionality is broad. This hypothesis was confirmed by estimating the nonlinear transfer function numerically for various directional spreading with an approximate solution of the Hasselmann integral. The development of the equilibrium spectral tail was examined. It was found that the spectral tail has developed, and the slope approached the Zakharov–Kolmogorof-type wave turbulence as the directionality broadened. The energy loss was not negligible in this case, suggesting that there was an energy cascade down to the high-frequency tail where the effect of viscosity dissipates the short waves, an essential ingredient in the establishment of the equilibrium spectrum. For the unidirectional case, the slope of the spectral tail was much steeper than that of the directionally broad cases. As the wave spectrum narrows, the relative significance of the four-wave resonance decreases; beyond a certain point, waves become unstable and the quasi-resonant interaction becomes dominant.

The observation of the wave evolution in an enclosed basin provided useful insight. However, because the wave motion is confined within a bounded body of water, the findings are suggestive if not conclusive. It is highly desirable to conduct a similar study in a basin of different geometry, both numerically and physically.

Acknowledgments. We thank H. Itakura for his assistance in conducting the experiment of the random wave evolution. We thank T. Lamont-Smith, H. Tomita, M. Onorato, A. Babanin, and M. Tanaka for their valuable comments on the paper. We also thank the two anonymous reviewers for their constructive comments. They helped improve the paper, particularly to isolate the effect of breaking dissipation and to quantify the dependency of the magnitude of the resonant interaction to the directional spreading. T. Waseda and T. Kinoshita were supported by the Grant-in-Aid for Scientific Research of the Japan Society for the Promotion of Science.

REFERENCES

Babanin, A. V., and Y. P. Soloviev, 1998: Variability of directional spectra of wind-generated waves, studied by means of wave staff arrays. *Mar. Freshwater Res.,* **49,** 89–101.

Badulin, S. I., A. V. Babanin, V. E. Zakharov, and D. Resio, 2007: Weakly turbulent laws of wind-wave growth. *J. Fluid Mech.,* **591,** 339–378.

Donelan, M. A., W. M. Drenan, and A. K. Magnussen, 1996: Nonstationary analysis of the directional properties of propagating waves. *J. Phys. Oceanogr.,* **26,** 1901–1914.

Gramstad, O., and K. Trulsen, 2007: Influence of crest and group length on the occurrence of freak waves. *J. Fluid Mech.,* **582,** 463–472.

Hara, T., and C. C. Mei, 1991: Frequency downshift in narrow-banded surface waves under the influence of wind. *J. Fluid Mech.,* **230,** 429–477.

Hasselmann, S., K. Hasselmann, J. H. Allender, and T. P. Barnett, 1985: Computations and parameterizations of the nonlinear energy transfer in a gravity-wave spectrum. Part II: Parameterizations of the nonlinear energy transfer for application in wave models. *J. Phys. Oceanogr.,* **15,** 1378–1391.

Hwang, P. A., and D. W. Wang, 2001: Directional distribution and mean square slopes in the equilibrium and saturation ranges of the wave spectrum. *J. Phys. Oceanogr.,* **31,** 1346–1360.

Janssen, P. A. E. M., 2003: Nonlinear four-wave interactions and freak waves. *J. Phys. Oceanogr.,* **33,** 863–884.

Komatsu, K., and A. Masuda, 1996: A new scheme of nonlinear energy transfer among wind waves: RIAM method-algorithm and performance. *J. Oceanogr.,* **52,** 509–537.

Melville, W. K., 1982: The instability and breaking of deep-water wave. *J. Fluid Mech.,* **115,** 165–185.

Onorato, M., A. R. Osborne, and M. Serio, 2002: Extreme wave events in directional, random oceanic sea states. *Phys. Fluids,* **14,** 25–28.

——, ——, ——, L. Cavaleri, C. Brandini, and C. T. Stansberg, 2004: Observation of strongly non-Gaussian statistics for random sea surface gravity waves in wave flume experiments. *Phys. Rev. E,* **70,** 067302, doi:10.1103/PhysRevE.70.067302.

——, and Coauthors, 2009: Statistical properties of mechanically generated surface gravity waves: A laboratory experiment in a three-dimensional wave basin. *J. Fluid Mech.,* **627,** 235–257.

Pushkarev, A., D. Resio, and V. Zakharov, 2003: Weak turbulent approach to the wind-generated gravity sea waves. *Physica D,* **184,** 29–63.

Soquet-Juglard, H., K. Dysthe, K. Trulsen, H. E. Krogstat, and J. Liu, 2005: Probability distribution of surface gravity waves during spectral changes. *J. Fluid Mech.,* **542,** 195–216.

Stiassnie, M., A. Regev, and Y. Agnon, 2008: Recurrent solutions of Alber's equation for random water-wave fields. *J. Fluid Mech.,* **598,** 245–266.

Tamura, H., T. Waseda, Y. Miyazawa, and K. Komatsu, 2008: Current-induced modulation of the ocean wave spectrum and the role of nonlinear energy transfer. *J. Phys. Oceanogr.,* **38,** 2662–2684.

Tanaka, M., 2001: Verification of Hassleman's energy transfer among surface gravity waves by direct numerical simulations of primitive equations. *J. Fluid Mech.,* **223,** 603–629.

Trulsen, K., and K. Dysthe, 1997: Frequency downshift in three-dimensional wave trains in a deep basin. *J. Fluid Mech.,* **352,** 359–373.

Tulin, M. P., and T. Waseda, 1999: Laboratory observations of wave group evolution, including breaking effects. *J. Fluid Mech.,* **378,** 197–232.

Waseda, T., T. Kinoshita, and H. Tamura, 2009: Evolution of a random directional wave and freak wave occurrence. *J. Phys. Oceanogr.,* **39,** 621–639.